J. Korean Earth Sci. Soc., v. 40, no. 4, p. 428–435, August 2019
https://doi.org/10.5467/JKESS.2019.40.4.428
ISSN 1225-6692 (printed edition)
ISSN 2287-4518 (electronic edition)

# Geoacoustic Model of Coastal Bottom Strata off the Northwestern Taean Peninsula in the Yellow Sea

**Woo-Hun Ryang[1,*], Hyuckjong Kwon[2], Jee-Woong Choi[2], Kyong-O Kim[3], and Jooyoung Hahn[4]**

[1]Division of Science Education and Institute of Science Education, Chonbuk National University, Jeonju 54896, Korea
[2]Department of Marine Science and Convergence Engineering, Hanyang University-ERICA, Ansan 15588, Korea
[3]Korea Institute of Geoscience and Mineral Resources (KIGAM), Daejeon 34132, Korea
[4]Agency for Defense Development, Jinhae 51678, Korea

**Abstract:** In the shallow coastal area, located off the northwestern Taean Peninsula of the eastern Yellow Sea, geoacoustic models with two layers were reconstructed for underwater acoustic experimentation and modeling. The Yellow Sea experienced glacio-eustasy sea-level fluctuations during Quaternary period. Coastal sedimentation in the Yellow Sea was characterized by alternating terrestrial and shallow marine deposits that reflected the fluctuating sea levels. The coastal geoacoustic models were based on data from piston, grab cores and the high-resolution 3.5 kHz, chirp seismic profiles (about 70 line-kilometers, respectively). Geoacoustic data of the cores were extrapolated down to 3 m in depth for geoacoustic models. The geoacoustic property of seafloor sediments is considered a key parameter for modeling underwater acoustic environments. For simulating actual underwater environments, the P-wave speed of the models was adjusted to *in-situ* depth below the sea floor using the Hamilton method. The proposed geoacoustic models could be used for submarine acoustic inversion and modeling in shallow-water environments of the study area.

Keywords: geoacoustic model, geoacoustic property, coastal geoacoustic, Yellow Sea

## 1. Introduction

The geoacoustic properties of seafloor sediments provide a key parameter for modeling the underwater acoustic environments. In the eastern Yellow Sea, although the geoacoustic data were partly published (Ryang et al., 2001; Ryang et al., 2019), it still lacks the data. The Yellow Sea experienced an impact of glacio-eustasy sea-level fluctuations during Quaternary (Lee et al., 2014; Li et al., 2016; Yoo et al., 2016a; Yoo et al., 2016b; Zhao et al., 2018). Coastal sedimentation on the Yellow Sea was characterized by alternating terrestrial and shallow marine deposits reflecting the fluctuating sea levels (Yang and Lin, 1991; Marsset et al., 1996; Cummings et al., 2016; Li et al., 2016; Liu et al., 2016; Zhao et al., 2018). This geological history resulted in a complex sedimentary accumulation.

This study focused on reconstructing a geoacoustic model of the coastal area where was located off the northwestern Taean Peninsua in the eastern Yellow Sea. Sediments of the study area comprise terrigenous and marine sediments in a shallow continental shelf (KIGAM, 1992; KIGAM, 2017). The geoacoustic model details surficial and subbottom sediment layers in the seafloor and the geoacoustic environmental parameters with measured, extrapolated, and predicted values (Hamilton, 1980; 1987). Coastal areas of shallow-water environments need a detailed geoacoustic model because they should reflect the complex sea bottom showing lateral and vertical variability of acoustic properties (Carey et al., 1995; Jackson and Richardson, 2007; Katsnelson et al., 2012). This study will provide

*Corresponding author: ryang@jbnu.ac.kr
Tel: +82-63-270-2790

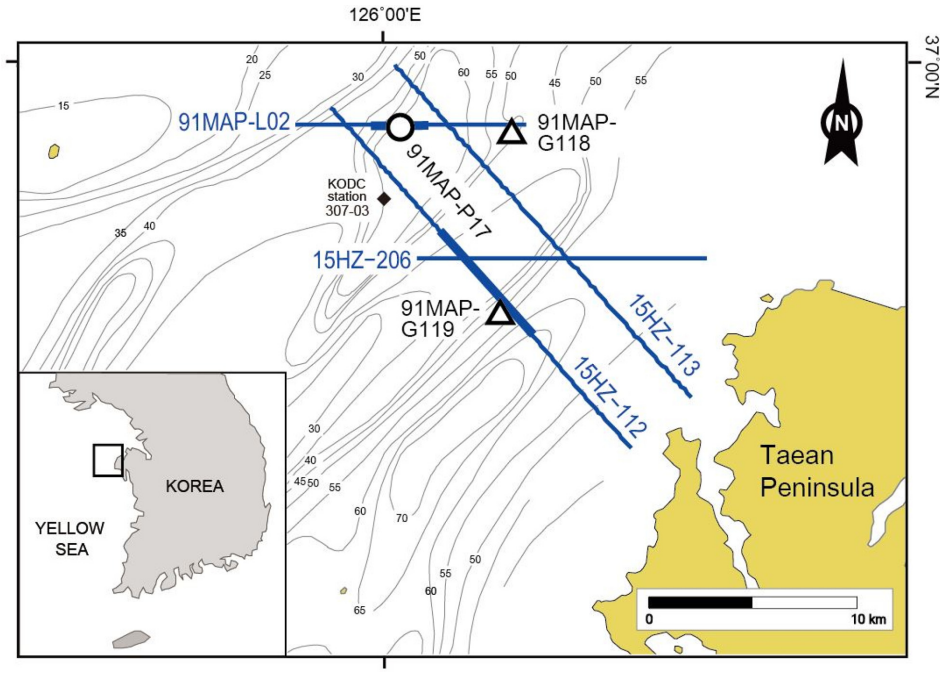


**Fig. 1.** (Color online) Geographic location and bathymetry of the study area, located off the Taean Peninsula in the western Yellow Sea (contours in meters) (modified after KIGAM, 1992; KIGAM, 2017). Location map of seismic lines, core sites, and water-mass measuring station of the Korea Oceanographic Data Center (KODC). Bold parts of the lines indicate the profiles of Line 91MAP-L02 shown in Fig. 2 and Line 15HZ-112 in Fig. 3, respectively.

geoacoustic models in the study area (Fig. 1) based on high-resolution seismic profiles and sedimentary cores acquired for geological researches. These models help understand the geoacoustic characteristics and fulfill acoustic works of underwater and sea bottom (e.g. Yoon et al., 2015).

## 2. Materials and Methods

A total of 70 line-kilometers of subbottom profiles (SBP) and chirp seismic profiles was used for reconstruction of the geoacoustic model (Figs. 1-3). The 3.5 kHz SBP was acquired by GeoPulse system (model 137D transducer, 5430A transmitter, and 5210A receiver) of the Korea Institute of Geology, Mining and Materials (KIGAM) using a main frequency of 3.5 kHz as a source signal (Fig. 2; KIGAM, 1992). The navigation of ship used the global positioning system (GPS), which speed was maintained at about 4-6 knot. Water depth was measured by single beams of 12 and 38 kHz (model EA500, SIMRAD). The chirp profiles were acquired by the chirp system of the Edgetech (USA) using a frequency range of 0.5 to 7.2 kHz (KIGAM, 2017). Both the shot interval and record time were 0.5 sec and the sampling interval was 0.046 ms. The navigation was precisely recorded by the differential global positioning system of space based augmentation system. Water depth was measured by multiple beams of 200, 300, and 400 kHz (model EM2040, Kongsberg Maritime).

This study is referred to core data of 1 piston core and 2 grab cores of the Van Veen grab sampler (Figs. 1, 4; Table 1), collected by the R/V Tamhae of KIGAM (KIGAM, 1992). Sediments in the piston and grab cores were sampled for size analysis. The grab and piston core samples were slabbed by acrylic sampler for X-ray radiographs. Grain-size distribution was analyzed using the standard dry-sieving method for the sand fraction (>63 $\mu$m) and using the pipette method for the mud fraction (<63 $\mu$m) (KIGAM,

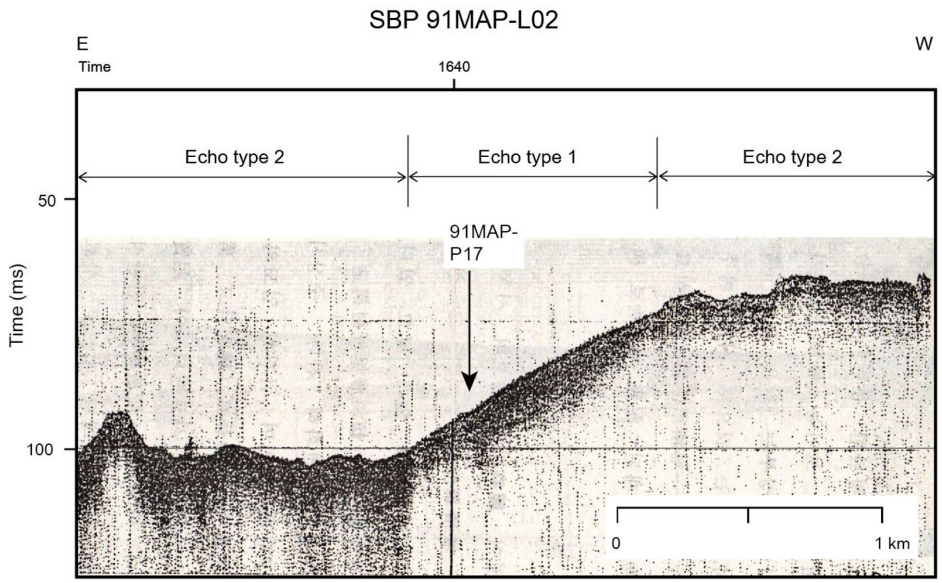


**Fig. 2.** 3.5 kHz SBP of 91MAP-L02 with core site of 91MAP-P17. See Fig. 1 for trackline. Vertical depth is expressed with two-way travel time in milliseconds.

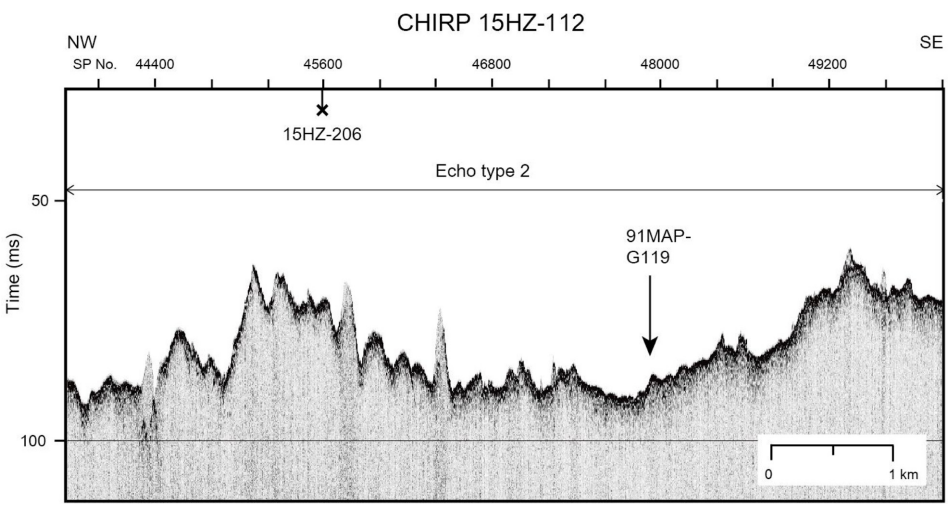


**Fig. 3.** Chirp profile of 15HZ-112 with core site of 91MAP-G119. See Fig. 1 for trackline. Vertical depth is expressed with two-way travel time in milliseconds

1992). The sediment type of textural parameters was classified by the scheme of Folk and Ward (1957) and Folk (1968). Temperature compensation and sound speed ratio for the *in-situ* speed followed the equation of Mackenzie (1981) using mean temperature and salinity of the water-mass database in a water depth of 0 and 50 m for 20 years (1995-2014), measured by the Korea Oceanographic Data Center (KODC) (Fig. 1; Table 1).

## 3. Regional Marine Geology

The Yellow Sea is a shallow epicontinental sea (average 55 m deep), semi-enclosed by the adjacent landmass of China and Korea (Fig. 1) (Chough et al., 2000). High-magnitude (>100 m) sea-level fall of the last glaciation event resulted in widespread regressive incisions on the almost entire shelf surface (Lee and

**Table 1.** Location, water depth, temperature, salinity, and p-wave speed of bottom water of 91MAP-P17, 91MAP-G118, and 91MAP-G119 core sites (see Fig. 1 for location). Geoacoustic and physical properties of the core sediments comprise *in-situ* P-wave speed and attenuation, sound speed ratio, wet density, mean grain size, porosity, and sediment type. Note that the *in-situ* P-wave speeds were calculated using the sound speed ratio of the Hamilton method (Hamilton, 1980)

| Geoacoustic Model no. | Latitude | Longitude | Line no. | | | | | | | |
|---|---|---|---|---|---|---|---|---|---|---|
| Water Depth (m) | Temp. *In-situ* (°C) | Salinity *In-situ* | Sea Water | Depth D (m) | Vp *In-situ* (m/s) | kp Attenuation (dB/kHz-m) | Wet Density (g/cm$^3$) | Mz $\Phi$ | Porosity % | Sediment Type Folk (1968) |
| | Stratigraphic Unit (SU) | Sound Speed Ratio (SSR) | Geoacoustic Unit (GU) | | | | | | | |
| 91MAP-P17 | 36.9727°N | 126.0098°E | 91MAP-L02 | | | | | | | |
| 61 | 12.0 | 31.6 | bottom water | | 1494 | | | | | |
| | 1 | 1.181 | GU 1 | 0 | 1764 | 0.47 | 2.05 | 2.1 | 39 | S |
| | 1 | 1.181 | GU 1 | 0.5 | 1764 | 0.47 | 2.05 | 2.1 | 39 | S |
| | 2 | 1.287 | GU 2 | 0.5 | 1923 | 0.62 | 2.15 | 0.63 | 34 | gS |
| | 2 | 1.287 | GU 2 | 3 | 1927 | 0.62 | 2.15 | 0.63 | 34 | gS |
| 91MAP-G118 | 36.9652°N | 126.0632°E | 91MAP-L02 | | | | | | | |
| 50 | 12.0 | 31.6 | bottom water | | 1494 | | | | | |
| | 1 | 1.169 | GU 1 | 0 | 1746 | 0.46 | 2.03 | 2.3 | 40 | S |
| 91MAP-G119 | 36.8995vN | 126.062°E | 15HZ-112 | | | | | | | |
| 50 | 12.0 | 31.6 | bottom water | | 1494 | | | | | |
| | 1 | 1.280 | GU 1 | 0 | 1912 | 0.61 | 2.14 | 0.7 | 34 | (g)S |

Yoon, 1997; Jin and Chough, 1998; Jin et al. 2002; Cummings et al., 2016; Yoo et al., 2016a; Yoo et al., 2016b). During the post-glacial sea-level rise, most of the lowstand incisions were almost filled with transgressive estuarine or terrigenous sediments, which were covered with the transgressive sand sheet formed during a later phase of the transgression (Lee and Yoon, 1997; Jin and Chough, 1998; Jin et al. 2002).

The study area is bounded on the east by the Korean coast and open westwards to the Yellow Sea with water depths ranging from 20 to 70 m (Fig. 1; KIGAM, 1992). It is located off the northwestern Taean Peninsua. The seafloor is characterized by a NE-SW trending ridge-and-swale topography (KIGAM, 1992). An apparent sediment source for the study area is the Han River emptying terrestrial sediment of 10-12×10$^6$ tons annually (Cummings et al., 2016).

## 4. Results

### 4.1. Seismic Data

Based on seafloor topography, surface bedforms, and acoustic characters of the 3.5 kHz SBP and chirp profiles, two echo types are identified in the study area. The echo type 1 is characterized by indistinct, very prolonged bottom echoes with no sub-bottom reflectors, which also shows relatively flat surface and sharp bottom echoes (Fig. 2). The relatively sharp bottom echoes reflect that the seafloor is covered with coarse-grained sediments such as sands. Partly deeper sound penetration suggests that the surface sediment comprises relatively fine-grained sediments such as a mixture of sands and silts (e.g. Damuth, 1980; Chough et al., 2002).

The echo type 2 consists of relatively flat or variable topographic seafloor, which was incised by a various scale of troughs or valleys. The very strong bottom echoes with poor sound penetration are interpreted that the seafloor comprises coarse-grained sediments such as gravelly sands. The small-scale troughs on the seafloor are interpreted as channels (e.g. Damuth, 1980; Chough et al., 2002). Shallow incision depths and poorly organized ubiquitous occurrences suggest that the surface deposits probably

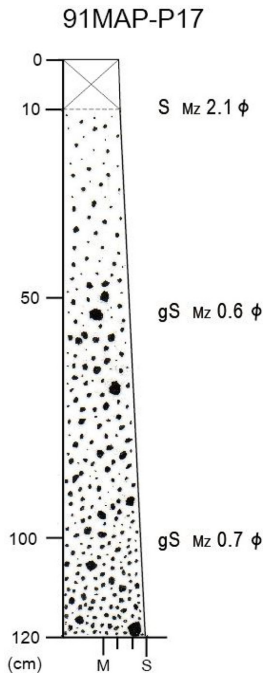


**Fig. 4.** Core lithology with sediment type and mean grain sizes of 91MAP-P17. For location, see Fig. 1. Sampling depth of sediment texture is shown in Table 1.

formed by strong tidal currents during the late stage of sea-level rise (Chough et al., 2002).

### 4.2. Sediment Data

The piston core of 91MAP-P17 (P17) penetrated into sediments of echo type 1 (Fig. 2), which depth is 120 cm at the water depth of 61 m. Core sediments of P17 show sediment types S and gS of the Folk scheme and moderately well sorted to poorly sorting ($\sigma_I$ 0.60 to 1.52 Φ) (Table 1; Folk, 1968; KIGAM, 1992). The sorting becomes poorer in the middle and lower parts of the core rather than that of the upper part (KIGAM, 1992). The mean grain sizes of sand range from 2.13 Φ to 0.69 Φ (Table 1). The sand and gravelly sand facies show a reddish yellow (7.5YR6/6) to olive gray (5Y6/8) color (KIGAM, 1992). The columnar section represents a fining-upward trend albeit the absence of 10 cm-thick sediments on the top (Fig. 4). The grab cores of 91MAP-G118 (G118) and 91MAP-G119 (G119) acquired sediments of echo type 2 (Fig. 3). The sediment of G118 shows sediment types S with mean grain size ($M_z$ 2.3 Φ) and sorting ($\sigma_I$ 0.99 Φ), and that of G119 shows (g)S with mean grain size ($M_z$ 0.7 Φ) and sorting ($\sigma_I$ 2.07 Φ) of the Folk scheme. The G119 sediment is indicative of a mixture of gravels and sands because the sorting value is very poorly sorted (Folk, 1968; KIGAM, 1992).

### 4.3. Physical and Geoacoustic Property

Physical and geoacoustic properties were calculated by regression equations of mean grain size because they were not measured at the time of experiment. The equations are made by recently measured data in the Yellow Sea (KIGAM, 2014; KIGAM, 2017). Physical properties consist of wet density and porosity and geoacoustic data comprise P-wave speed and attenuation and sound speed ratio. P-wave speed values are calculated using this equation (Table 1).

$$\text{P-wave speed (m/s)} = 8.199\ M_z^2 - 130.73\ M_z + 2042.9 \quad (1)$$

where $M_z$ is mean grain size (Φ). The regression equation was based on 868 sets of measured P-wave speed and mean grain size in the Yellow Sea (KIGAM, 2014; KIGAM, 2017; Ryang et al., 2019). The attenuation of P-wave speed was calculated by the regression equation of $k=0.697e^{-0.183Mz}$ (Jackson and Richardson, 2007). The attenuation value is 046–0.62 dB/kHz-m (Table 1).

The P-wave speed of sediments divided by that of the bottom water is the sound speed ratio (Table 1; Hamilton, 1980). The speed of the bottom water was calculated by the equation of Mackenzie (1981) using the KODC dataset (Fig. 1). Wet bulk density is in a range of 2.03–2.15 g/cm$^3$ and porosity is 34-40% (Table 1). It was obtained using the regression equations, based on 1304 datasets of measured wet bulk density, porosity, and mean grain size, respectively (KIGAM, 2014; KIGAM 2017; Ryang et al., 2019).

### 4.4. Geoacoustic Model

The study area was located on the shallow coastal area off the northwestern Taean Peninsula in the western Yellow Sea, which seafloor consists of terrigenous

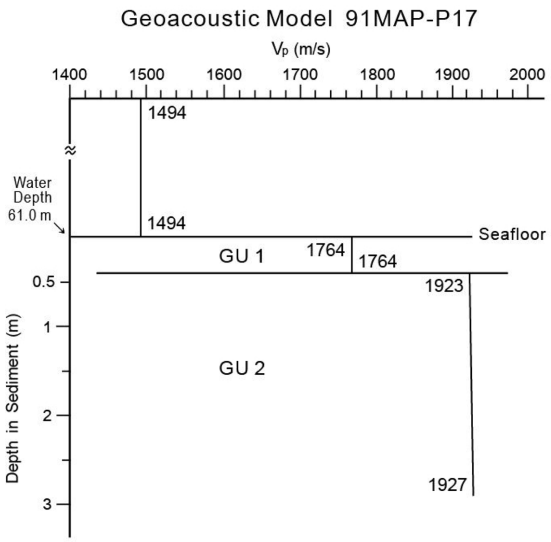


**Fig. 5.** Geoacoustic Model of the 91MAP-P17 core site. For location, see Fig. 1.

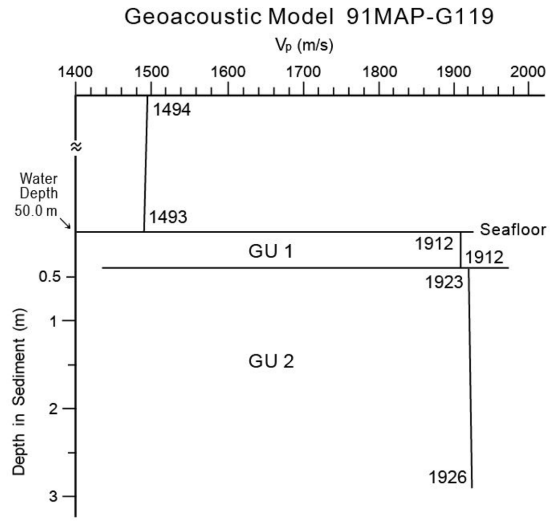


**Fig. 6.** Geoacoustic Model of the 91MAP-G119 core site. For location, see Fig. 1.

and marine coarse-grained sediments (KIGAM, 1992; KIGAM, 2017). Based on the seismic profiles, sediment, and acoustic data, the geoacoustic models were reconstructed as two-layer models of surficial and sub-bottom geoacoustic units (Figs. 5, 6). Each geoacoustic unit was also representative of physical and geoacoustic environmental parameters with measured, extrapolated, and predicted values through the Hamilton modeling (Table 1; e.g. Hamilton, 1980). This study suggests three geoacoustic models of two layers representing the study coastal area (Table 1).

## 5. Discussion

In the eastern Yellow Sea, coastal sedimentation in the shallow-water environments experienced a complex depositional history by the sea-level changes (Chough et al., 2002; Jin et al., 2002; Shinn et al., 2007). In this area, the reconstruction of a geoacoustic model should consider the stratigraphic and bottom models reflecting lateral and vertical variability of acoustic properties. This study provided three geoacoustic models through the Hamilton modeling in the study area using high-resolution seismic profiles and sedimentary cores, acquired for geological researches (Table 1; Figs. 5, 6). The data were combined for reconstructing the models because the P17 core were defective in the surface sediments and those of the G118 and G119 cores could not acquire sub-bottom sediments. On the other hand, reconstruction of the models was based on lateral and vertical interpretation of the SBP and chirp profiles. The vertical interpretation also suggests that the geoacoustic models are available to about 3 m depth in sediment below the seafloor.

In addition, it is difficult to measure P-wave speed of the coarse-grained sediment such as gravelly sand or sandy gravel in the laboratory experiment (Jackson and Richardson, 2007). The reason is that wavelengths of the transmitted pulse maintained at several hundred kHz-1 MHz are shorter than the largest grain size of the specimen (Kolsky, 1963). This study used the experienced and regression equation for the calculated values, based on 868 sets of P-wave speed and mean grain size and 1304 datasets of wet bulk density, porosity, and mean grain size, measured in the Yellow Sea. In the shallow-water environments of the coast study area, our suggested geoacoustic models might be used for acoustic inversion and modeling.

## 6. Conclusions

In the shallow coastal area, located off the northwestern Taean Peninsula of the eastern Yellow Sea, geoacoustic models of two layers were reconstructed for underwater acoustic experiment and modeling. The models were based on the data of the high-resolution 3.5 kHz and chirp seismic profiles with cores. Geoacoustic data of the cores were extrapolated down to 3-m depth of the geoacoustic models. For actual underwater experiments, the P-wave speed of the models was compensated to *in-situ* depth below the sea floor using the Hamilton method.

In the study area, the coastal bottom strata were characterized by relatively coarse-grained deposits of a mixture of sand and gravel, originated from terrestrial and shallow marine environments. Based on the regression equation of 868 sets of P-wave speed and mean-grain-size data, measured in the Yellow Sea, the geoacoustic properties were calculated (Table 1). In the echo type 1 of seismic profile, geoacoustic model of P17 ($M_z$ 2.1 Φ) represented *in-situ* P-wave speed of 1764 m/s, whereas geoacoustic model of G119 ($M_z$ 0.7 Φ) in the echo type 2 showed relatively faster P-wave speed of 1912 m/s.

## Acknowledgments

The data of marine geophysics and geology were acquired and processed by the Korea Institute of Geoscience and Mineral Resources. We are grateful to anonymous reviewers for their critical and helpful comments. WHR thanks Ms. Kang, Sol-Ip (Chonbuk National University) for working the computer graphics. This work was supported by the Agency for Defense Development of Korea (ADD) grant (UD170014DD) and by the National Research Foundation of Korea (NRF) grant funded by the Korea government (MSIT) (NRF-2019R1F1A1057715).

## References

Carey, W.M., Doutt, J., Evans, R.B., and Dillman, L.M., 1995, Shallow-water sound transmission measurements on the New Jersey continental shelf. IEEE Journal of Oceanic Engineering, 20, 321-336.

Chough, S.K., Kim, J.W., Lee, S.H., Shinn, Y.J., Jin, J.H., Suh, M.C., and Lee, J.S., 2002, High-resolution acoustic characteristics of epicontinental sea deposits, central-eastern Yellow Sea. Marine Geology, 188, 317-331.

Chough, S.K., Lee, H.J., and Yoon, S.H., 2000, Marine geology of Korean seas. Elsevier, Amsterdam, 313 p.

Cummings, D.I., Dalrymple, R.W., Choi, K, and Jin, J.H., 2016, The tide-dominated Han river delta, Korea, Elsevier, Amsterdam, Netherlands, 376 p.

Damuth, J.E., 1980, Use of high-frequency (3.5-12 kHz) echograms in the study of near-bottom sedimentation processes in the deep-sea: a review, Marine Geology, 38, 51-75.

Folk, R.L., 1968, Petrology of sedimentary rocks. Hemphill's, Austin, USA, 170 p.

Folk, R.L. and Ward, W.C., 1957, A study in the significance of grain-size parameters. Journal of Sedimentary Petrology, 27, 3-27.

Hamilton, E.L. 1980, Geoacoustic modeling of the sea floor. Journal of the Acoustical Society of America, 68, 1313-1339.

Hamilton, E.L., 1987, Acoustic properties of sediments. In Lara-Saenz, A., Ranz-Guerra, C., and Carbo-Fite, C. (eds.), Acoustics and Ocean Bottom. Cosejo Superior de Investigaciones Cientificas, Madrid, Spain, 3-58.

Jackson, D.R. and Richardson, M.D., 2007, High-frequency seafloor acoustics. Springer, New York, USA, 616 p.

Jin, J.H. and Chough, S.K., 1998, Partitioning of transgressive deposits in the southeastern Yellow Sea: a sequence stratigraphic interpretation. Marine Geololgy, 149, 79-92.

Jin, J.H., Chough, S.K., and Ryang, W.H., 2002, Sequence aggradation and systems tracts partitioning in the ME Yellow Sea: roles of glacio-eustasy, subsidence and tidal dynamics. Marine Geology, 184, 249-271.

Katsnelson, B., Petnikov, V., and Lynch, J., 2012, Fundamentals of shallow water acoustics. Springer, New York, USA, 540 p.

KIGAM (Korea Institute of Geology, Mining and Materials), 1992, Marine geological study of the continental shelf off Taean, west coast, Korea. KIGAM Research Report KR-91-5C, 216 p.

KIGAM (Korea Institute of Geology, Mineral and Materials), 2014, Geological characterization of recent muddy sediment for reservoir potential, and in-situ analysis of shallow gas. KIGAM Research Report GP2012-005-2014(3), 370 p.

KIGAM (Korea Institute of Geology, Mineral and Materials), 2017, Study on the coastal geohazard factors analysis, west coast, Korea. Oceans and Fisheries R&D

Report R&D/2011-0016, 1161 p.

Kolsky, H., 1963, Stress waves in solids. Dover Publications, New York, 224 p.

Lee, G.S., Kim, D.C., Yoo, D.G., and Yi, H.I., 2014, Stratigraphy of late Quaternary deposits using high resolution seismic profile in the southeastern Yellow Sea. Quaternary International, 344, 109-124.

Lee, H.J. and Yoon, S.H., 1997, Development of stratigraphy and sediment distribution in the northeastern Yellow Sea during Holocene sea-level rise. Journal of Sedimentary Research, 67, 341-349.

Li, X.S., Zhao, Y.X., Feng, Z.B., Liu, C.G., Xie, Q.H., and Zhou, Q.J., 2016, Quaternary seismic facies of the South Yellow Sea shelf: depositional processes influenced by sea-level change and tectonic controls. Geological Journal, 51, 77-95.

Liu, S., Li, P., Feng, A., Du, J., Gao, W., Xu, Y., Yu, X, Li, P., and Nan, X., 2016, Seismic and core investigation on the modern Yellow River Delta reveals the development of the uppermost fluvial deposits and the subsequent transgression system since the postglacial period. Journal of Asian Earth Sciences, 128, 158-180.

Mackenzie, K.V., 1981, Nine-term equation for sound speed in the oceans. Journal of the Acoustical Society of America, 70, 807-812.

Marsset, T., Xia, D., Berne, S., Liu, Z., Bourillet, J.F., and Wang, K., 1996, Stratigraphy and sedimentary environments during the late Quaternary in the Eastern Bohai Sea (North China Platform). Marine Geololgy, 135, 97-114.

Ryang, W.H., Jin, J.H., and Hahn, J., 2019, Geoacoustic model at the YSDP-105 long-core site in the mid-eastern Yellow Sea. The Journal of the Korean Earth Sciences Society, 40, 24-36.

Ryang, W.H., Jin, J.H., Jang, S.H., Kim, S.P., Kim, H.T., Lee, C.W., Chang, J.H., and Choi, J.H., 2001, Geoacoustic characteristics of Quaternary stratigraphic sequences in the mid-eastern Yellow Sea. The Sea. Journal of the Korean Society of Oceanography, 6, 81-92.

Shinn, Y.J., Chough, S.K., Kim, J.W., and Woo, J., 2007, Development of depositional systems in the southeastern Yellow Sea during the post glacial transgression. Marine Geology, 239, 59-82.

Yang, Z. and Lin, H., 1991, Quaternary processes in eastern China and their international correlation. A Report by the IGCP 218 Chinese Working Group. Geological Publishing House, Beijing, 139 p.

Yoo, D.G., Chang, T.S., Lee, G.S., Kim, G.Y., Kim, S.P., and Park, S.C., 2016a, Late Quaternary seismic stratigraphy in response to postglacial sea-level rise at the mid-eastern Yellow Sea. Quaternary International, 392, 125-136.

Yoo, D.G., Lee, G.S., Kim, G.Y., Kang, N.K., Yi, B.Y., Kim, Y.J., Chun, J.H., and Kong, G.S., 2016b, Seismic stratigraphy and depositional history of late Quaternary deposits in a tide-dominated setting: an example from the eastern Yellow Sea. Marine and Petroleum Geology, 73, 212-227.

Yoon, Y.G., Lee, C., Choi, J.W., Cho, S., Oh, S., and Jung, S.K., 2015, Measurements of mid-frequency bottom loss in shallow water of the Yellow Sea. The Journal of the Acoustical Society of Korea, 34, 423-431.

Zhao, W., Zhang, X., Wang, Z., Chen, S., Wu, Z. and Mi, B., 2018, Quaternary high-resolution seismic sequence based on instantaneous phase of single-channel seismic data in the South Yellow Sea, China. Quaternary International, 468, 4-13.

Manuscript received: July 28, 2019
Revised manuscript received: August 21, 2019
Manuscript accepted: August 22, 2019